Available online at www.sciencedirect.com
ScienceDirect
Journal of the European Ceramic Society 31 (2011) 3055–3062
www.elsevier.com/locate/jeurceramsoc

Synthesis and properties of mullite-type $(Bi_{1-x}Sr_x)_2(M^1{}_{1-y}M^2{}_y)_4O_{9-x}$ (M = Al, Ga, Fe)

Thorsten M. Gesing [a,b,*], Reinhard X. Fischer [a], Manfred Burianek [c], Manfred Mühlberg [c], Tapas Debnath [b,1], Claus H. Rüscher [b], Jan Ottinger [c], J.-Christian Buhl [b], Hartmut Schneider [a,c]

[a] FB05 Kristallographie, Universität Bremen, Klagenfurter Straße, D-28359 Bremen, Germany
[b] Institut für Mineralogie, Universität Hannover, Callinstraße 3, D-30167 Hannover, Germany
[c] Institut für Kristallographie, Universität Köln, Greinstraße 6, D-50939 Köln, Germany

Available online 4 May 2011

Abstract

Mullite-type $A_2M_4O_9$ phases (M = Al, Ga, Fe), representing promising oxygen conducting materials for solid oxide fuel cells (SOFCs), were synthesized using the glycerine- and the EDTA/citric acid synthesis method. For strontium-doped material pure phases could be obtained only by washing the samples after the heating in both synthesis methods. Temperature dependent investigations were carried out to show the influence of the metal atoms on the structural stability and thermal expansion coefficients. Whereas the Sr-free phases show a quasi linear thermal expansion behavior in all three directions up to their incongruent melting points, a discontinuity in the measured range is observed for the investigated strontium doped dibismuth-nonaoxotetrametallate(III) caused by the decomposition into $Bi_2M_4O_9$, strontium metallates and bismuthoxide. Big single crystals were only observed for the Sr-free compound, of which the structure of $Bi_2(Ga_{0.45}Fe_{0.55})_4O_9$ will be presented here in the Bärnighausen tree corresponding mullite-type setting.

Keywords: Mullite-type compounds; Thermal expansion; Glycerine method; EDTA/citric acid method; Crystal structure

1. Introduction

$Bi_2M_4O_9$ compounds with mullite-like structures[1] have been considered as a suitable model system for the investigation of oxygen mobility. These compounds show a large variety of chemical compositions[2–7] some of which can be obtained as large single crystals.[8] Some of these materials show remarkable ion conductivity[7] having potential as electrolytes in solid oxide fuel cells (SOFC) or oxygen sensors.[6,9] They show high emissions in the range of red light, which may be utilized as high energy scintillation detectors.[10,11]

Various methods are described for their synthesis. Arpe and Müller-Buschbaum[12] reported on firing a mixture of stoichiometric quantities of the corresponding binary oxides at temperatures up to 1273 K to obtain powder samples. Niizeki and Wachi[2] got single crystals of dimension 0.5 mm × 0.3 mm × 0.3 mm using an excess of Bi_2O_3 which was heated at 1173 K for 12 h followed by a cooling rate of 7 K/h down to 1073 K; they extracted the solidified mass with hot nitric acid. Small single crystals were reported to be produced by melting a previously sintered oxide mixture using a CO_2-laser at around 1273 K.[3] Large crystals of 20 mm × 20 mm × 10 mm were grown using the top-seeded solution-growth (TSSG) method.[8] Zha et al.[7] described a combustion method where the metal nitrates were mixed with glycine (glycine to metal ratio = 2:1). After the explosion the samples were heated for 2 h at 1023 K to prepare powder samples which were then pressed to pellets and heated between 1323 K and 1363 K to obtain dense ceramic bodies. We reported in a conference contribution[13] on the synthesis of these phases using the glycerine method; almost parallel to Voll et al.[14] where the use of glycerine as solvent was also described as a successful method. Additionally, the synthesis of the mullite-related bismuth compounds using the EDTA/citric acid method is described. This method was successfully used, for example, for the formation of BSCF perovskite-type samples suitable for cathode materials in SOFC's.[15,16]

For the application of $A_2M_4O_9$ mullite-type compounds in SOFC's the suitable phases should be stable up to a temperature of about 1200 K without showing any phase transition or

* Corresponding author at: Chemische Kristallographie fester Stoffe, Universität Bremen, LeobenerStraße/NW2, D-28359 Bremen, Germany. Tel.: +49 421 218 65171; fax: +49 421 218 98 65171.
E-mail address: gesing@uni-bremen.de (T.M. Gesing).
[1] Present address: Chemistry Department, Dhaka University, Bangladesh.

0955-2219/$ – see front matter © 2011 Elsevier Ltd. All rights reserved.
doi:10.1016/j.jeurceramsoc.2011.04.004

decomposition. Additionally, it is of certain importance to know the thermal expansion behavior of such compounds, to exclude thermal breaking caused by mechanical stress of the formed body. To investigate this behavior, in situ temperature dependent X-ray diffraction measurements were necessary which were evaluated by structure refinements using the Rietveld method for data collected on powder samples. The results concerning a systematic investigation of thermal stability and thermal expansion are outlined here.

$Bi_2M_4O_9$ compounds belong to the family of mullite-type structures.[1] They are described to crystallize in a subgroup (space group *Pbam*) of the tetragonal mullite aristotype (space group *P4/mbm*) of index 4, in contrast to mullite itself which belongs to a subgroup of index 2 (also *Pbam*).[1] Therefore the atomic coordinates of the $Bi_2M_4O_9$ phases used in this paper are transformed into a standardized model derived from the aristotype. The structure itself is characterized by chains of edge sharing MO_6 octahedra. These chains are interconnected by M_2O_7 double tetrahedral units and BiO_6E groups (where E refers to $6s^2$ lone electron pair) in an alternate and ordered manner along the *c*-axis. Because of the lone-pair electrons of the bismuth ions every second possible oxygen position along this *c*-axis is unoccupied.[2] This position was proposed by Abrahams et al.[6] to be used by neighboring oxygen atoms as a jump position in a cooperative motion of these oxygen atoms as a mechanism of ion conductivity. Investigating the electrical behavior, Bloom et al.[17] found conductivity values of 1 S/m at 800 °C for $Bi_2Al_4O_9$. This value was reported[7] to be increased to 28 S/m at 800 °C for $(Bi_{1-x}Sr_x)_2Al_4O_{9-x}$ with *x* equal to 0.2.

2. Experimental

For the formation of the title compounds two different synthesis paths, the glycerine and the EDTA/citric acid method, were chosen. Using the glycerine method for the preparation of $Bi_2Al_4O_2$, as an example, 8.09 mmol $Bi(NO_3)_3{\cdot}5H_2O$ and 16.18 mmol $Al(NO_3)_3{\cdot}9H_2O$ (total metal nitrate amount of 10 g) were mixed with glycerine (1,2,3-propantriol). Ten weight% glycerine of the total amount of the metal nitrates was added (here 1 g) to dissolve the metal nitrates under magnetic stirring placing the glass beaker used in an oil bath at 353 K. During this heating process the metal nitrates first dissolved in glycerine and increased the amount of total liquid by releasing crystal water. The metal-nitrate decomposition was observed due to the release of brown gases (NO_x) together with the evaporation of water. The release of NO_x led to the formation of a paste, becoming more and more viscous. After half an hour the glass beaker was placed into a furnace for about 2 h at 473 K. During this heating period additional NO_x gases and water were released resulting in dry foam. Notably, the appearance of the foam differed depending on the amount of glycerine used during the synthesis. As more glycerine is used the more the foam volume increases. The foam could be ground to a fine powder which was nearly X-ray amorphous. It still contained some nitrate groups and organic components as confirmed by infrared (IR) investigations (therefore it is called NCO-gel). This gel was placed in a platinum crucible and heated at 1023 K for several hours or days to obtain a well-crystallized powder of the dibismuth-nonaoxometallate. After washing the samples using diluted nitric acid pure phases were observed.

In the EDTA/citric acid method the metal atoms are dissolved and captured in the EDTA chelate complex resulting in a clear aqueous solution. For this synthesis 5 mmol $Bi(NO_3)_3{\cdot}5H_2O$ were added to 15 ml deionized water and stirred. To this solution 10 mmol $Al(NO_3)_3{\cdot}9H_2O$ were added under stirring followed by 22.5 mmol citric acid (1.5 times the mole sum of the metal components). Now the solution became nearly clear. Still stirring, 15 mmol EDTA (mole sum of the metal components) and 15 ml NH_3 (25%) were added resulting in a colorless clear solution. After adding 100 ml water a pH value of 9.5 was measured which decreased to 6.5 while boiling the solution for 5.5 h. During this time the clear solution changed to a brownish syrupy mass which turned to a black powder while heating at 473 K for 12 h. The black powder was transferred to a platinum crucible and heated at 1023 K for 48 h. Finally, a pale yellow powder was observed identified as pure $Bi_2Al_4O_2$ by X-ray powder diffraction investigation. Remarkably, the pale yellow color observed here was less intense than the color observed after the synthesis using the glycerine method heating a sample at 1023 K and 48 h. After washing the sample with diluted nitric acid, the samples were white, showing that the reasons for the yellow sample color after heating is originated by small amounts of non-crystalline Bi_2O_3. For the strontium doped samples an appropriate amount of Bi-salt was replaced by $Sr(NO_3)_2$ in both methods. For comparison strontium doped samples were also prepared as described by Zha et al.[7] using the combustion method. Nevertheless, it was also not possible to obtain pure strontium doped samples after the heating process. All samples were washed in diluted nitric acid to remove the impurity phases, especially, Bi_2O_3 and $SrAl_2O_4$ which were always present. Attempts to synthesize large scale single crystals of the strontium-doped sample by the top seeded solution growth (TSSG) method,[8] which we have successfully used here for the growth of $Bi_2(Ga_{1-x}Fe_x)_4O_9$, failed in any case for crystals with more than approximately 100 ppm Sr.

X-ray diffraction measurements were carried out for all synthesized products followed by structure refinements using the "Diffrac^{Plus} Topas 4.2" (Bruker AXS GmbH, Karlsruhe) software for the Rietveld refinements of the powder data. These data were collected on a Panalytical MPD powder diffractometer in Bragg-Brentano geometry equipped with a secondary Ni filter, $CuK\alpha_{1,2}$ radiation and a X'Celerator detector. Temperature dependent experiments were performed with the same instrument and geometry adapting a Paar-HTK1200N heating chamber in the diffractometer. The finely grained powder was mixed with acetone, transferred to the corundum sample holder and mounted in the heat chamber after drying. Data collection was done starting at 298 K in steps of 50 K from 332 K up to 1272 K and then with the same steps down to room temperature again. In the case of the strontium-doped samples some runs were carried out twice with the same sample to check for further changes. For the description of the reflection profiles the fundamental parameter approach implemented in the refinement program was used, fitting the fundamental parameters to a LaB_6 standard powder for each configuration. Up to

five background parameters were refined together with a parameter for the sample displacement. For all background fits the Chebychev function was used. Additionally, phase parameters such as scale factor and lattice parameters of the mullite-related phases were also refined. Lorentzian and Gaussian parameters were optimized for the average crystal size and the micro strain. For the single crystal data collection of $Bi_2(Ga_{0.45}Fe_{0.55})_4O_9$ a Stoe IPDS1 diffractometer was used, rotating the crystal around phi by 1° for each frame in a total frame range from −6° to 360°, exposing each frame for 3 min. The collection of the integrated intensities was performed using the software package provided with the diffractometer. After refining an orthorhombic unit cell, a numerical absorption correction has been applied for the space group *Pbam*, refining the shape and distance of the measured crystal surfaces. For the structure refinement with the Shelx program[18] the starting model published by Niizeki and Wachi[2] was used assuming a mixed occupation of gallium and iron on the metal atom positions. Spectroscopic measurements in the mid-infrared (MIR) regions were carried out on a Bruker IFS66 spectrometer using the KBr and PE method. The samples were ground to an average particle size of ∼1 μm. All IR spectra are plotted in absorption units (A.U.) according to $-\ln(I/I_O)$ (I, I_O = transmitted intensity of the sample plus KBr and pure KBr discs, respectively). Themogravimetric (TG) and Differential Thermal Analysis (DTA) measurements were carried out in a Setaram Setsys 1750 Evolution instrument to investigate the decomposition of the synthesized gel. The decompositions of the compounds with mixed metal content were measured using a Netsch STA413 instrument. For these measurements a heating rate of 10 K/min was used together with a flow of 20 ml/min of synthetic air.

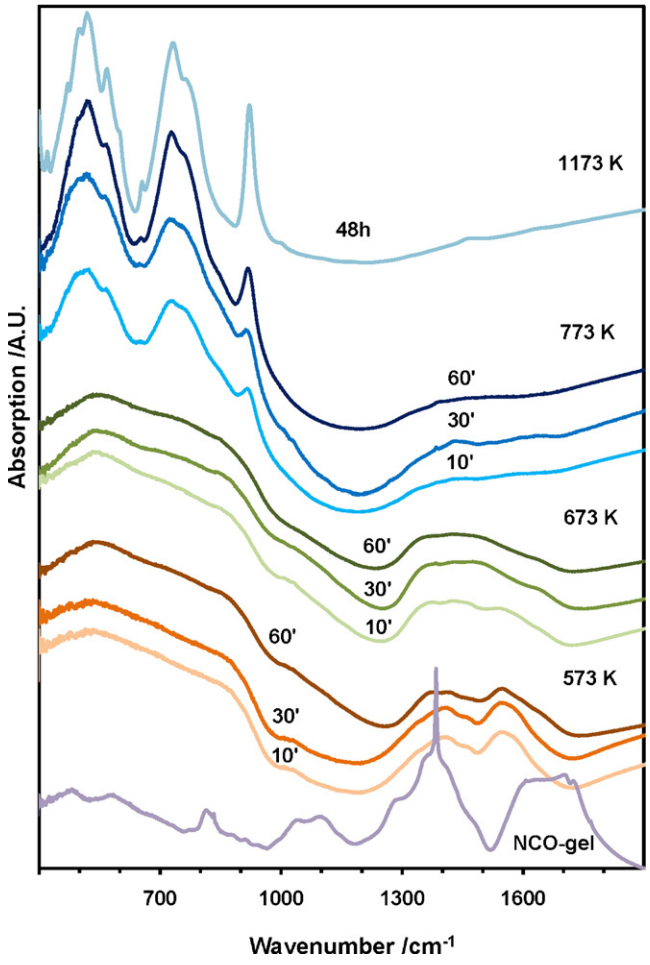

Fig. 1. Infrared spectra of $Bi_2Al_4O_9$ of gel (bottom) formed at 80 °C, different heating steps and well-crystallized sample (top).

3. Results and discussion

3.1. Powder synthesis

The synthesis of the mullite-type $Bi_2M_4O_9$ phases was reported in the past to be possible in various ways.[2–8] In all these synthesis attempts temperatures were used which were above the melting point of Bi_2O_3 resulting in well-crystallized samples which were mainly reported to be single crystals, pure powders or dense ceramic bodies. Repeating the combustion method for the synthesis of strontium-doped dibismuth-nonaoxoaluminate as reported by Zha et al.,[7] who heated the synthesis mixture in an intermediate step below the melting point of bismuthoxide, phase purity could never be observed. The impurities could be removed by washing the samples with diluted nitric acid which yielded white powders. We have pressed these powders into pellets and heated them at 1323 K for 2 h. After this heating process yellow ceramic bodies showing a relative density greater than 85% were observed. The yellow color originated in small amounts of Bi_2O_3. This phase was also detected in well-resolved X-ray powder patterns as small amounts of $SrAl_2O_4$. To get pure samples the glycerine as well as the EDTA/citric acid method were tested for the synthesis. Unfortunately, for the strontium-doped samples neither method was able to produce pure samples after heating the powder above 1000 K. The best purity of the as-synthesized samples was achieved by the EDTA/citric acid method as indicated by the yellow color being very slight. Nevertheless, these samples also showed impurities and had to be washed with nitric acid. Additionally, this synthesis is a bit more complicated and time consuming with respect to the glycerine method. Therefore we synthesized all other powder samples via the glycerine method. Using this method, samples were heated at different temperatures and time to investigate the decomposition of the NCO-gel and the formation of the mullite-type compound using infrared spectroscopy. As shown in Fig. 1, NO_3 modes (around 1400 cm^{-1}) as well as modes from organic components (above 1500 cm^{-1}) could be observed at 573 K and 673 K without significant intensity loss for all samples heated for 10 min to 1 h. Additionally, no modes were observed yet which would indicate the formation of $Bi_2Al_4O_9$. After heating the samples at 773 K for 1 h nearly all nitrate and organic modes could not be observed anymore but modes belonging to $Bi_2Al_4O_9$ could be seen even while heating the sample for 10 min at this temperature, becoming more pronounced with time as shown by the comparison with the IR spectra of a well crystallized sample (Fig. 1). However, the samples changed to dark grey after heating at 773 K for 1 h. Thermal analysis of a homogenized sample after the first synthesis step of 353 K shows (Fig. 2) the loss of water

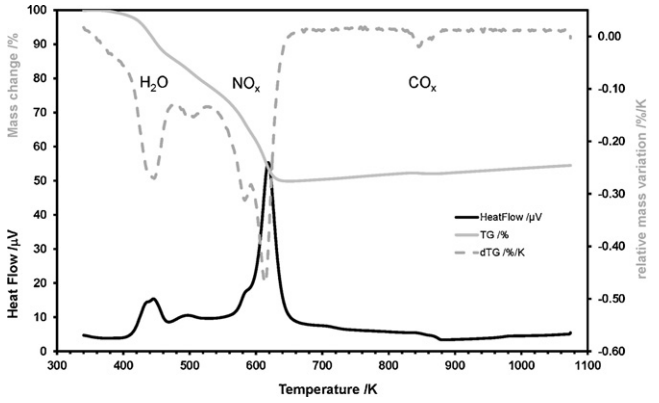

Fig. 2. Thermal analysis of a $Bi_2Al_4O_9$ NCO-gel. The measured mass change is given together with the sample heat flow (exothermal signals point upwards). For better comparison the first derivate of the mass change (relative mass variation) is additionally plotted.

and nitrate groups up to approximately 660 K. Another signal at around 850 K was observed which is interpreted as a loss of CO and/or CO_2 as a result of the reaction of pure carbon with the synthetic air in the experiment. The carbon itself is formed during the reduction of the glycerine at lower temperatures explaining the appearing grey color of the initially white powder in the heating experiments. Out of these investigations the lowest temperature for the synthesis should be 873 K, the highest 1090 K, at least for strontium-doped samples, to rule out melting of Bi_2O_3. To obtain well-crystallized samples a synthesis temperature of 1023 K was chosen for the strontium-doped samples. For the strontium-free samples the synthesis temperature was fixed right below the incongruent melting point of the compounds taking the melting point of the less stable end-member when compounds with mixed metal atoms were synthesized.

3.2. Single crystal investigations

Additionally to the powder samples with mixed metal position occupation, big single crystals (Fig. 3) were observed using the TSSG method. For this crystal growth a molar ratio of Ga_2O_3 to Fe_2O_3 of 1 was used which results in a crystal composition of $Bi_2(Ga_{0.45(2)}Fe_{0.55(2)})_4O_9$, refined from single-crystal X-ray data and confirmed by EDX-analysis, indicating a slight preference for iron to be incorporated into the structure (Fig. 4). Such a behavior was not observed for powder samples where the whole batch was transferred to the product. Refinement details of the single crystal structure investigation are given in Table 1. The atomic positional parameters (Table 2) were refined in agreement with the structure setting derived from the aristotype as explained by Fischer and Schneider.[1] Single crystal neutron diffraction[19] refinements might indicate that the space group *Pbam* is not correct for the description of this mullite-type compound structure. We have not observed any violation of the systematic absence rules for the X-ray data set used for the current refinement greater than three standard deviations. Nevertheless, the large anisotropic displacement parameter of the O3 position plotted in Fig. 4b is in agreement with the slight off-centering of this atomic position refined from neutron data for $Bi_2Fe_4O_9$.[19] The metal atoms in this compound are octahedrally coordinated (M1) by oxygen atoms showing distances of 194.8(5) pm (x2 O12), 201.9(5) pm (x2 O2) and 203.0(5) pm (x2 O11), respectively, as well as tetrahedrally coordinated (M2) with M–O distances of 180.0(1) pm (O3), 184.2(7) pm (O12 and 187.9(7) pm (x2 O2). Typical for this structure-type are the rather short M2–O3–M2 distances in the double-tetrahedra units which are also observed here and which are correlated with a much larger anisotropic displacement parameter for the O3 position. For the bismuth atoms four close oxygen atoms (213,2(7) pm x2 O2, 215.0(7) pm O11 and 246.5 (7) pm O11) are observed

Fig. 3. Single crystals of $Bi_2(Ga_{1-x}Fe_x)_4O_9$ obtained using the TSSG single-crystal growth method, with dimensions of $20 \times 20 \times 10\,mm^3$.

Table 1
Crystallographic and X-ray data of $Bi_2(Ga_{0.45(2)}Fe_{0.55(2)})_4O_9$.

Space group	*Pbam*
a/pm	796.48(6)
b/pm	835.02(8)
c/pm	593.93(4)
$V/10^6$ pm^3	395.0(1)
Formula units/unit cell	$Z=2$
Calculated density/(g cm^3)	6.836
Crystal dimensions (mm^3)	$0.15 \times 0.12 \times 0.08$
Effective mosaic spread	0.012
Radiation	Mo Kα
h, *k*, *l* range	±11, ±11, −7 to 8
2θ max./°	60.60
Absorption correction	Numerical
Reflections measured	8675
Refinement software	Shelx
Reflections observed	4545
Residual (merge) R_{int}	0.0704
Residual (intensity) R_{sigma}	0.0416
Var. positional parameters	46
Residual R_1 (all)	0.035
Residual R_1 (gt)	0.027
Weighted residual wR_2 (all)	0.066
Weighted residual wR_2 (gt)	0.065
CSD-No.[a]	422829

[a] Further details are available from the FIZ Karlsruhe, Gesellschaft für wissenschaftlich-technische Information mbH, D-76344 Eggenstein-Leopoldshafen, Germany, referring to the no. CSD, names of authors and citation of the paper.

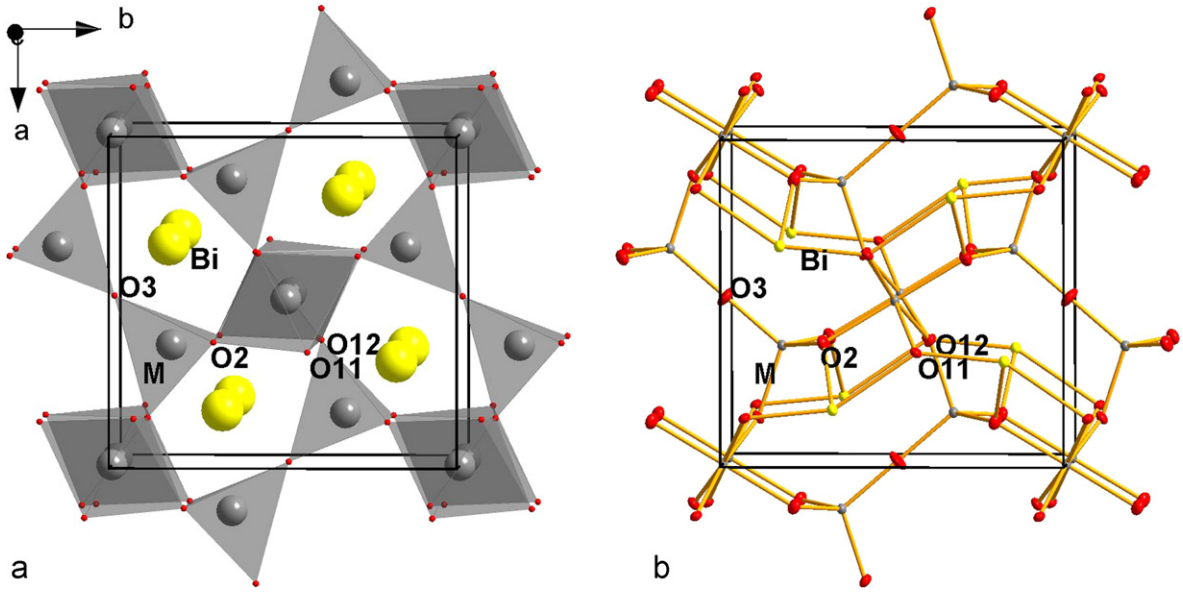

Fig. 4. Crystal–structure plot of $Bi_2(Ga_{1-x}Fe_x)_4O_9$ in polyhedral representation (left) and with interatomic bonds together with anisotropic atomic displacement ellipsoids (right).

together with 2 more distant oxygen atoms (300.2(6) pm x2 O2) giving a 4 + 2 coordination (Fig. 4) in which the lone $6s^2$ electron pair has to be taken into account. These bismuth atoms and the M_2O_7 double-tetrahedra units stabilize the structure by interconnecting the M^1O_4 octahedral chains which are orientated parallel the *c*-axis.

Table 2
Refined atomic parameters of $Bi_2(Ga_{0.45(2)}Fe_{0.55(2)})_4O_9$ ($U_{eq} = (U_{11} + U_{22} + U_{33})/3$ given in 10^{-4} pm^2).

Atom	*Pbam*	Variable	Refined value
Bi	4g	*x*	0.32409(5)
		y	0.17319(4)
		U_{eq}	0.0119(2)
M1[6]	4e	*z*	0.25831(24)
		occ. Ga[a]	0.355(36)
		U_{eq}	0.0081(5)
M2[4]	4h	*x*	0.14781(15)
		y	0.33694(14)
		occ. Ga[a]	0.550(38)
		U_{eq}	0.0090(5)
O11	4g	*x*	0.35046(89)
		y	0.42938(86)
		U_{eq}	0.0111(16)
O12	4h	*x*	0.36762(94)
		y	0.40545(89)
		U_{eq}	0.0127(17)
O2	8i	*x*	0.13007(71)
		y	0.20721(56)
		z	0.24256(134)
		U_{eq}	0.0150(12)
O3	2d	U_{eq}	0.0347(39)

[a] occ.(Fe) = 1.0 − occ(Ga).

3.3. Thermal expansion

We have investigated the thermal expansion behavior of $Bi_2M_4O_9$ with M equal to Al, Ga, and Fe as well as mixed occupations of the M position for the series $Bi_2(Al_{1-x}Fe_x)_4O_9$ and $Bi_2(Ga_{1-x}Fe_x)_4O_9$ with steps of $x = 0.1$ each (Fig. 5). Generally all these compounds show the same behavior. Up to 1272 K, which is the highest temperature reached during the temperature-dependent investigations, no phase transition was observed. During the heating and cooling runs of the samples the observed lattice parameters are the same for each temperature step (within the standard deviation). In Fig. 6, the *c* lattice parameters calculated for the respective temperatures for the heating and cooling run of a $Bi_2Al_4O_9$ powder samples are given as an example. As shown in Fig. 6, the thermal expansion is not strictly linear; it could be better described with a quadratic function. For the calculation of the thermal expansion of each lattice parameter, the lattice parameter difference between room-temperature and the actual temperature was calculated by dividing the lattice parameter difference with the room-temperature value which was then multiplied with the reciprocal temperature difference: $\Delta e/e\ 1/\Delta T$ with *e* as lattice parameter *a*, *b*, or *c* or the unit cell volume *V*. In Fig. 5 the expansion parameters between 298 K and 1272 K are given for the mixed systems. In case of the $Bi_2(Al_{1-x}Fe_x)_4O_9$ mixed samples it seems that the thermal expansion is dominated by the influence of the aluminum in this compound which is most pronounced in the behavior of the *b* lattice parameter which is nearly constant until *x* increases above 0.50. As we observe the highest thermal expansion in this lattice direction also the volume expansion is dominated by this effect. The expansion of the *c* parameter is almost constant, only slightly increasing for iron contents above around 90%. The expansion of the *a* parameter changes linearly with the composition and is always lower than the other two expansions. For the *b* and *c* directions the same thermal expansion is observed at an

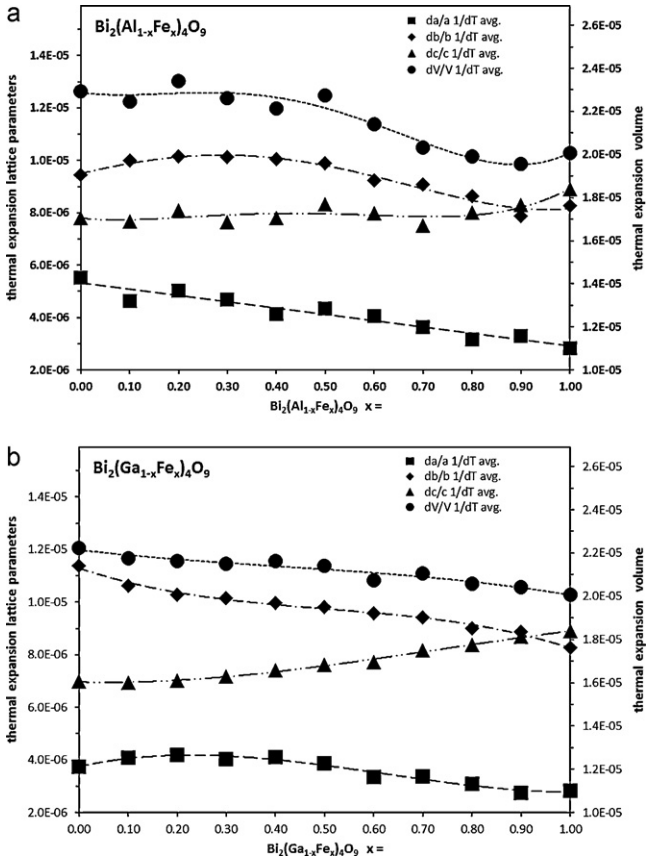

Fig. 5. Thermal expansion values for the series $Bi_2(Al_{1-x}Fe_x)_4O_9$ (top) and $Bi_2(Ga_{1-x}Fe_x)_4O_9$ (bottom).

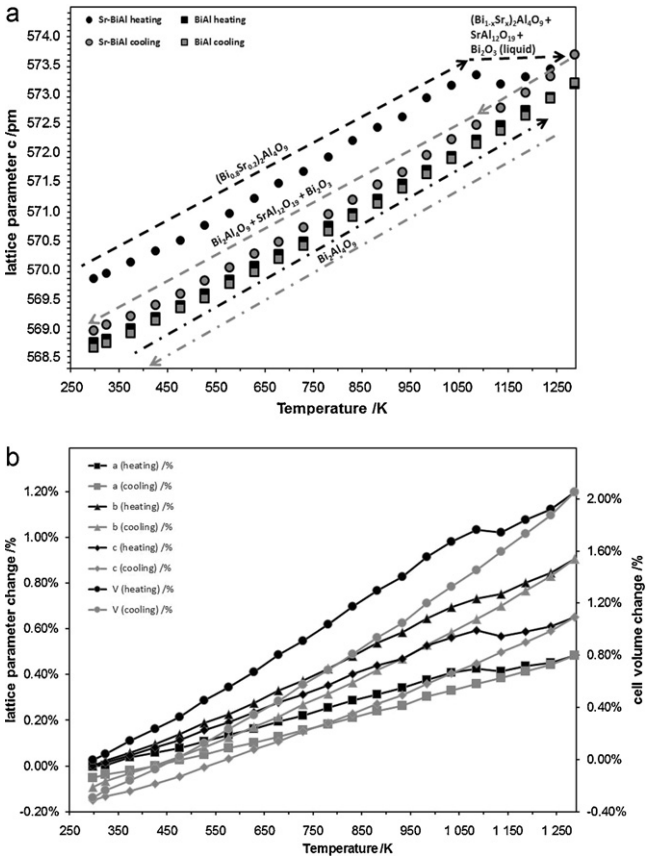

Fig. 6. Temperature dependency of the c lattice parameter of $Bi_2Al_4O_9$ (BiAl) and a powder sample with an initial composition of $(Bi_{0.8}Sr_{0.2})_2Al_4O_9$ (top) and relative change of the lattice parameters of the latter sample (bottom).

approximate composition of $x = 0.90$. For the $Bi_2(Ga_{1-x}Fe_x)_4O_9$ compounds the change in the thermal expansions of the different directions could be regarded as nearly linear with respect to the change of the chemical composition. Only the a direction behavior is probably slightly dominated by the gallium atoms. Because of the strong deviation of the composition-dependent thermal-expansion behavior of the $Bi_2(Al_{1-x}Fe_x)_4O_9$ series we have additionally investigated their change in the incongruent melting points (Fig. 7). This temperature is more or less constant from $x = 0$ up to $x = 0.7$. Above this iron content the incongruent melting point decreases to the value observed for the pure ferrate. This means, that the thermal stability and also the thermal expansion of these compounds is mainly dominated by the aluminum atoms incorporated in the structure.

3.4. Strontium doping effects

A completely different behavior is observed when bismuth in these phases is partially replaced by strontium during the synthesis. Additionally, an effect of the impurity phases is observed after the final heating step. Heating an as-synthesized sample with an initial strontium content of 20 mol%, a thermal expansion behavior up to 900 K is observed similar to that of a pure $Bi_2Al_4O_9$ phase. The only differences are slightly increased lattice parameters, most pronounced in the c direction (Fig. 6). As shown in Fig. 8(top) a small deviation could be observed between the expansion behavior of an as-synthesized sample and the corresponding washed sample beginning at this temperature. At 1073 K the change in the c lattice parameter could clearly be seen. This decrease of the lattice parameter is correlated with the appearance of $SrAl_{12}O_{19}$, as observed in the X-ray powder pattern, and additionally Bi_2O_3 (or a strontium doped variety of this compound) appears during the cooling runs below 1073 K when it starts to crystallize out of its melt. The decrease of the lattice parameter is (nearly) linear during the cooling run. A second

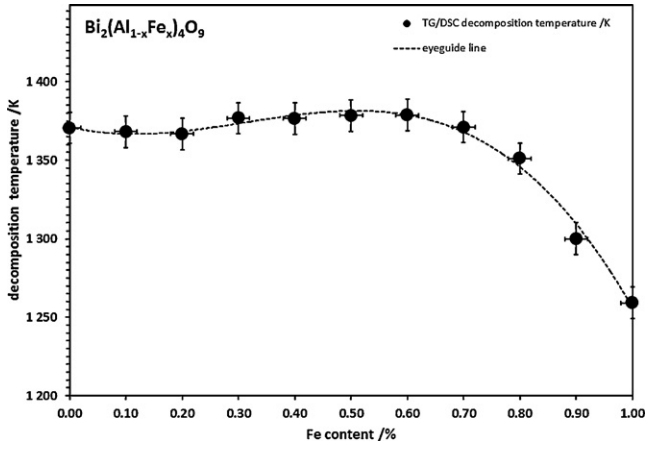

Fig. 7. Incongruent melting temperatures of $Bi_2(Al_{1-x}Fe_x)_4O_9$ compounds.

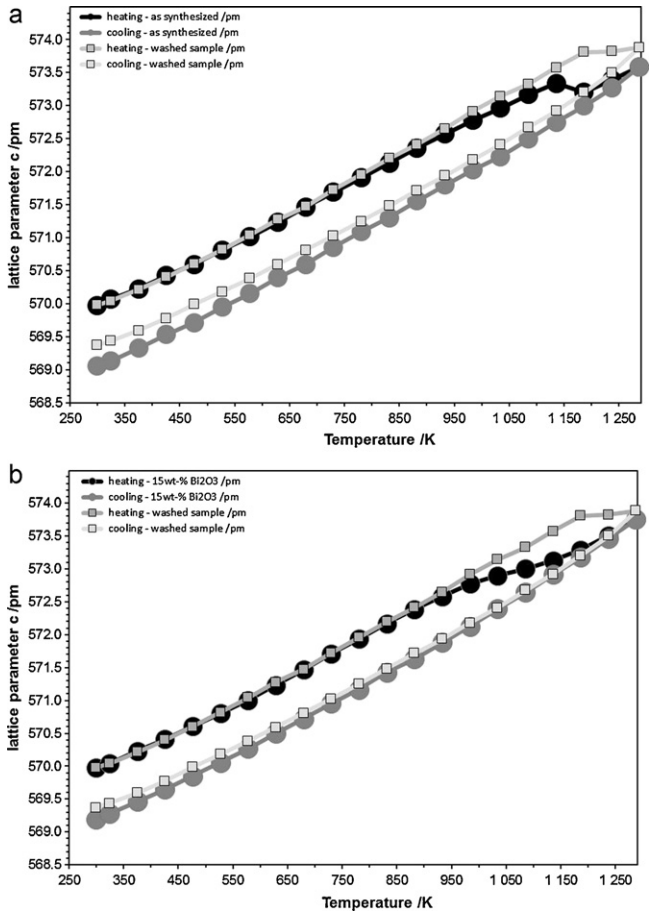

Fig. 8. Thermal behavior of the *c* lattice parameter observed for powder samples with an initial composition of $(Bi_{0.8}Sr_{0.2})_2Al_4O_9$. Top: Temperature cycle of a sample as synthesized compared with a washed sample (lighter color). Bottom: Temperature cycle of a washed sample (lighter color) compared with the same sample containing additional 15 wt% Bi_2O_3.

heating and cooling cycle with the identical sample reproduces the thermal behavior of the first cooling run. This means that no further deviation from the expected thermal expansion behavior is observed. The observed lattice parameters of the first cooling run and the second temperature cycle are nearly the same as for the Sr-free compound; these small deviations seems to show the differences for the identical phase between two different measurements. Because the structural effect of the strontium-doped sample is observed around the melting point of Bi_2O_3 this measurement was compared to a second one carried out with the same sample which was additionally washed with diluted nitric acid to remove all impurities, especially Bi_2O_3. As could be seen in the top graph of Fig. 8, the washed sample is more stable, a beginning decomposition is observed at around 1173 K. For this comparison the lattice parameters of the washed sample measured at 298 K before heating were set equivalent to the lattice parameters of the as-synthesized sample to see the small deviations. Obviously the plotted *c* lattice parameter of the washed sample is slightly smaller if one assumes that the decomposed phase is pure $Bi_2Al_4O_9$, which should have the same lattice parameter in both measurements. To be sure that this shift effect is correlated with the melting of Bi_2O_3 we have added 15 wt% Bi_2O_3 to the washed sample, mixed them carefully and repeated the experiment (Fig. 8(bottom)). It can be clearly seen that the decomposition temperature for the Bi_2O_3 containing sample decreases dramatically. On the other hand, the effect is observed to start at around 973 K which is approximately 100 K below the melting point of Bi_2O_3. This means that the diffusion potential of bismuth in this mixture is at 973 K high enough to initiate the decomposition of the strontium-doped sample. The increased decomposition temperature of the washed sample on the other hand could be interpreted as a nearly complete removement of "free" Bi_2O_3. The really small amounts probably left in the sample start to decompose the strontium-doped phase locally. This leads to an increasing amount of Bi_2O_3 which speeds up the decomposition more and more until the whole sample is transferred. This needs much more time than for a sample with higher Bi_2O_3 contents. We carried out the measurement in a way that each step lasts around one hour, which leads to a higher observed decomposition temperature. This effect is best observed for the **c** lattice-parameter but could also be seen in the other two directions as shown in the bottom graph in Fig. 6, where the relative lattice parameter changes are given with respect to the room-temperature values before a temperature cycle is started. It could be clearly deduced that all three lattice parameters decrease during the decomposition. This clearly shows that a strontium-doped bismuthaluminate is only stable up to approximately 1073 K, above this temperature it decomposes to the pure bismuthaluminate, hibonite ($SrAl_{12}O_{19}$) and Bi_2O_3 (which might be strontium doped). If it is assumed that all strontium in the hibonite was originated in the strontium doped bismuth-aluminate, a total of 5(3) mol% strontium in $(Bi_{1-x}Sr_x)Al_4O_{9-x}$ could be calculated using the weight fraction of hibonite from the Rietveld refinements for this calculation.

4. Conclusion

$Bi_2M_4O_9$ phases with M = Al, Ga, Fe could easily and quickly be prepared using the glycerine method. Nevertheless, pure samples could only be observed if an additional washing step with diluted nitric acid was applied. Strontium doped phases could not be observed if the samples were heated above the melting point of Bi_2O_3. This was also true for washed samples; it takes only more time to get a total decomposition. The decomposition could be seen on the appearance of hibonite as a marker. The hibonite could also be used to calculate the approximate strontium content in $(Bi_{1-x}Sr_x)Al_4O_{9-x}$. This leads to the fact that strontium doped single crystals could not be grown out of a melt as it is possible for pure bismuth metallates with mixed metal occupation in large scales. These pure bismuth mullite-type phases show a nearly linear thermal expansion behavior which could be observed without any phase transition up to their incongruent melting point. The thermal expansion as well as the incongruent melting is dominated by aluminum in the case of mixed aluminum/iron sample. If gallium is used instead of aluminum a dominance of gallium concerning the phase stability could be assumed as inferred from the thermal expansion along the *a* direction, but is not pronounced.

Another important point is that the increase of electrical conductivity described by Zha et al.[7] for an increasing amount of strontium during the synthesis of $(Bi_{1-x}Sr_x)Al_4O_{9-x}$ could not be related to an increase of defects in the mullite type phase, because the samples reported in Ref. [7] were all synthesized at temperatures more than 200 K above the decomposition temperature of the strontium doped mullite-type phase. Probably the increased conductivity could be explained with the increasing content of (strontium doped?) δ-Bi_2O_3, but this must be proven elsewhere.

Acknowledgements

We gratefully acknowledge the "Deutsche Forschungsgemeinschaft" for financial support in the projects GE1981/2-1, FI442/14-1 and MU1006/8-1 as part of the joint project PAK279.

References

1. Fischer RX, Schneider H. The mullite-type family of crystal structures. In: Schneider H, Komarneni S, editors. *Mullite* Weinheim: Wiley-VCH; 2005. pp. 1–46 and 128–140.
2. Niizeki N, Wachi M. The crystal structures of $Bi_2Mn_4O_{10}$, $Bi_2Al_4O_9$ and $Bi_2Fe_4O_9$. *Z Kristallogr* 1968;**127**: 173–87.
3. Müller-Buschbaum HK, Charles de Beaulieu D. Zur Besetzung von Oktaeder- und Tetraederpositionen in $Bi_2Ga_2Fe_2O_9$. *Z Naturforsch* 1978;**33b**:669–70.
4. Tutov AG, Markin VN. Izvestiya Akademii Nauk SSSR. *Neorg Mater* 1970;**6**:2014–7.
5. Giaquinta DM, Papaefthymiou GC, Davis WM, zur Loye H-C. Synthesis, structure, and magnetic properties of the layered bismuth transition metal oxide solid solution $Bi_2Fe_{4-x}Ga_xO_9$. *J Solid State Chem* 1992;**99**: 120–33.
6. Abrahams I, Bush AJ, Hawkes GE, Nunes T. Structure and oxide ion conductivity mechanism in $Bi_2Al_4O_9$ by combined X-ray and high-resolution neutron powder diffraction and ^{27}Al solid state NMR. *J Solid State Chem* 1999;**147**:631–6.
7. Zha S, Cheng J, Liu Y, Liu X, Meng G. Electrical properties of pure and Sr-doped $Bi_2Al_4O_9$ ceramics. *Solid State Ionics* 2003;**156**:197–200.
8. Schreuer J, Burianek M, Mühlberg M, Winkler B, Wilson DJ, Schneider H. Crystal growth and elastic properties of orthorhombic $Bi_2Ga_4O_9$. *J Phys Condens Matter* 2006;**18**:10977–88.
9. Goodenough JB. Oxide ion electrolytes. *Ann Rev Mater Res* 2003;**33**:91–128.
10. Blasse G, Boen Ho O. On the luminescence of bismuth aluminate ($Bi_2Al_4O_9$). *J Lumin* 1980;**21**:165–8.
11. Volkov VV, Egorysheva A. V. Photoluminescence in fast-response $Bi_2Al_4O_9$ and $Bi_2Ga_4O_9$ oxide scintillators. *Opt Mater* 1996;**5**:273–7.
12. Arpe R, Müller-Buschbaum H-K. Zur Kristallstruktur von $Al_4Bi_2O_9$. *J Inorg Nucl Chem* 1977;**39**:233–5.
13. Gesing Th M, Rüscher C. H. Spektroskopische und Röntgen-Einkristalluntersuchungen an $Bi_2Fe_4O_9$. *Z Kristallogr Suppl* 2006;**24**:176.
14. Voll D, Beran A, Schneider H. Variation of infrared absorption spectra in the system $Bi_2Al_{4-x}Fe_xO_9$ ($x = 0$–4), structurally related to mullite. *Phys Chem Miner* 2006;**33**:623–8.
15. Shao Z, Yang W, Cong Y, Dong H, Tong J, Xiong G. Investigation of the permeation behavior and stability of a $Ba_{0.5}Sr_{0.5}Co_{0.8}Fe_{0.2}O_{3-\delta}$ oxygen membrane. *J Membr Sci* 2000;**172**:177–88.
16. Arnold M, Gesing Th M, Martynczuk J, Feldhoff A. Correlation of the formation and the decomposition process of the BSCF perovskite at intermediate temperatures. *Chem Mater* 2008;**20**:5851–8.
17. Bloom I, Hash MC, Zebrowski JP, Myles KM, Krumpelt M. Oxide-ion conductivity of bismuth aluminates. *Solid State Ionics* 1992;**53-56**:739–47.
18. Sheldrick GM. A short history of SHELX. *Acta Crystallogr* 2008:112–22. A64.
19. Gesing TM, Nénert G, Burianek M, Mühlberg M, Schneider H, Fischer RX. Temperature-dependent single-crystal neutron diffraction investigations on mullite type $Bi_2Fe_4O_9$. In: Annual conference of the Deutsche Mineralogische Gesellschaft. Coll. Abstracts; 2010. P8,07.